# NUMERICAL SIMULATIONS OF HYDRODYNAMICALLY INTERACTING GRANULAR PARTICLES

Kengo Ichiki and Hisao Hayakawa
*Department of Physics, Tohoku University, Sendai 980-77, Japan*

# 1. INTRODUCTION

## 1.1 Granular Flow

Granular systems are typical objects of non-equilibrium statistical physics. Because granular particles are large enough to neglect the Brownian force and to be affected by the external force (gravity).

Although these granular materials consist of simple components which are granular particles and surrounding fluid, they show a large variety of phenomena.

## 1.2 Phenomena

### *"Fluidized bed"* [1,2]

In an experiment of fluidized beds, we prepare a vessel containing granular particles and impose a gas flow from the bottom of the vessel. As the flow rate changes, the system show various kinds of behaviors.

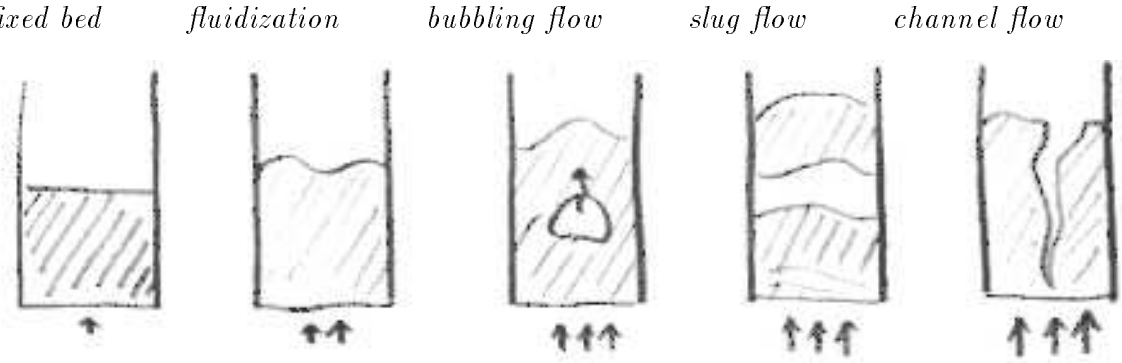

In this systems, it is obvious that **hydrodynamic effect** has an important role.

*"Pipe flow"*

Pipe flow is the simplest system of granular flows, in which granular particles is falling in a narrow pipe.

Even in such a simple system, it is observed in experiments that the uniform flow of particles is unstable and density waves appear [3–5]. In addition the fluctuation of density show $1/f^{\alpha}$ spectra [5].

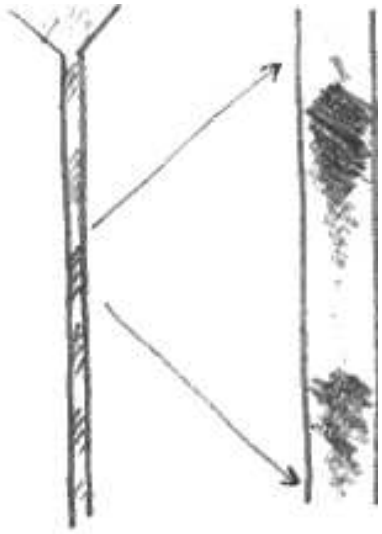

Pipe flows have been studied as the collection of inelastic particles (without hydrodynamics). However, in the experiments, it is found that the formation of density waves are closely related to the fluid flow in the pipe.

## 1.3 Hydrodynamic Effect

Here we focus on the hydrodynamic effects in granular flows.

One can expect naturally that the hydrodynamic effects of fluid surrounding particles must play an important role in the phenomena. It is sufficient to remember a simple example that one particle is falling down by the gravity. Situation is more difficult in granular flows, because the hydrodynamic effects depend on the density of particle significantly [6].

In this poster, we consider granular flows taking account of hydrodynamic effects numerically.

# 2. SIMULATION METHOD

In this section we presents the simulation method that take account of hydrodynamic interactions [7].

## 2.1 Properties of System

We neglect the complexities of granular systems, which are

- polydispersity
- direct interactions among the particles
  - the Coulomb interaction
  - intermolecular forces
- chemical reactions induced by mixing
- etc ... ,

but we treat the systems as which

- contain **monodisperse spheres**
- with **hard-core interactions**
- and with **hydrodynamic interactions**.

We define the following dimensionless quantities,

| | |
|---|---|
| Péclet number | $Pe = \dfrac{6\pi\mu a^2 \mathcal{V}}{k_B T}$ |
| Reynolds number | $Re = \dfrac{\rho_f a^3 \mathcal{V}^2}{\mu a^2 \mathcal{V}} = \dfrac{\rho_f a \mathcal{V}}{\mu}$ |
| Stokes number | $St = \dfrac{m\mathcal{V}^2}{6\pi\mu a^2 \mathcal{V}} = \dfrac{2}{9}\dfrac{\rho_p a \mathcal{V}}{\mu}$ |

$a$, $\rho_p$, $\rho_f$ and $\mu$ are the particle radius, the mass densities of the particle and the fluid, and the shear viscosity of the fluid respectively, $k_B$ is the Boltzmann's constant. $\mathcal{V}$ is the characteristic velocity, where we choose the sedimentation rate of one particle

$$\mathcal{V} = \frac{m\tilde{g}}{6\pi\mu a} = \frac{2a^2\rho_p\tilde{g}}{9\mu} \tag{1}$$

where $\tilde{g} = g(\rho_p - \rho_f)/\rho_p$.

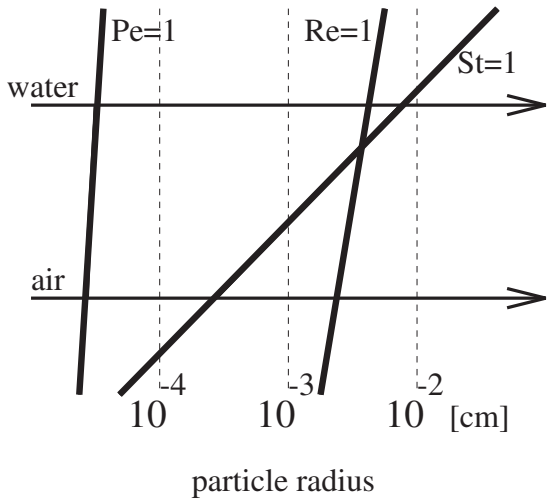


FIG. 1. Relation between the particle radius and dimensionless parameters.

Let us estimate the parameters when $\rho_p = 2.5$ [g cm$^{-3}$], which is a typical value of glass beads, and fluid is air and water. Relation between the radius and parameters is shown in Fig. 1. The lines in this figure connect the points where the parameters are equal to unity for air and water.

- $Pe \ll 1$ : the Brownian force is dominant
- $Pe \gg 1$ : the Brownian force is negligible

- $Re \ll 1$ : the fluid-inertia is negligible

- $Re \gg 1$ : the fluid-inertia is not negligible

- $St \ll 1$ : the particle-inertia is negligible
- $St \gg 1$ : the particle-inertia is important

## 2.2 Equation of Motion

In the case $Pe \ll 1$, particles with mass $m$ in a fluid obey the equation of motion,

$$m\frac{d}{dt}\mathbf{U} = \mathbf{F}_f + \mathbf{F}_g \tag{2}$$

where the velocity $\mathbf{U}$, the position $\mathbf{x}$ and the forces $\mathbf{F}_l$ $(l = f, g, i, b)$ represent vectors containing $N$ particle elements as

$$\mathbf{U} = \begin{bmatrix} \mathbf{U}^{(1)} \\ \vdots \\ \mathbf{U}^{(N)} \end{bmatrix}, \quad \mathbf{x} = \begin{bmatrix} \mathbf{x}^{(1)} \\ \vdots \\ \mathbf{x}^{(N)} \end{bmatrix}, \quad \mathbf{F} = \begin{bmatrix} \mathbf{F}^{(1)} \\ \vdots \\ \mathbf{F}^{(N)} \end{bmatrix}, \tag{3}$$

where the superscript $(i)$ represents the index of the particle. Two kinds of forces in (2) are

- $\mathbf{F}_f$ is the drag force from the fluid
- $\mathbf{F}_g$ is the gravitational force.

The hard-core collisions are treated as the exchange of the velocities with the restitution coefficient $e = 1$ which shows elastic and no dissipation.

We neglect the rotational motion of particles for simplicity.

## 2.2 Hydrodynamic Interaction

The most relevant and complicated force is $\mathbf{F}_f$, which is determined under the suitable boundary condition by the Navier-Stokes equation

$$\rho_f \left\{ \partial_t \mathbf{u} + (\mathbf{u} \cdot \nabla)\mathbf{u} \right\} = \mu \nabla^2 \mathbf{u} - \nabla p, \tag{4}$$

$$\nabla \cdot \mathbf{u} = 0. \tag{5}$$

The incompressibility is valid even if the fluid is air, when the particle motion is much slower than the sound velocity of fluid.

Hydrodynamic interaction among particles in the fluid are well understood only in the limiting cases,

- High Reynolds number, irrotational limit ($Re \gg 1, \nabla \times \mathbf{u} = 0$)
- Low Reynolds number limit ($Re \ll 1$).

In the granular flow, it is expected that the viscous force from the fluid has an important role, we adopt the latter limit ($Re \ll 1$). In this limit the Navier-Stokes equation is reduced to the Stokes equation

$$-\mu \nabla^2 \mathbf{u} + \nabla p = \vec{0}, \tag{6}$$

and the particle velocity $\mathbf{U}$ is connected with the force induced on the particles by the fluid $\mathbf{F}_f$ through the resistance matrix $\mathbf{R}(\mathbf{x})$ [8,9],

$$\mathbf{F}_f = -\mathbf{R}\left(\mathbf{x}\right) \cdot \left(\mathbf{U} - \mathbf{u}^{\infty}\right), \tag{7}$$

where $\mathbf{u}^{\infty}$ is the fluid velocity in the absence of particles. $\mathbf{R}$ depends only on the instantaneous particle configuration $\mathbf{x}$. R is calculated by the Stokesian dynamics method [10] which take account of both lubrication effect and long range effect.

Then the non-dimensional form of Eq. (2) is reduced to

$$St\frac{d}{dt}\mathbf{U}(t) = -\mathbf{R}(\mathbf{x}(t)) \cdot (\mathbf{U}(t) - \mathbf{u}^{\infty}) - \mathbf{E}_z. \tag{8}$$

Here we scale the velocities by $\mathcal{V}$, the length by the radius $a$ and the resistance matrix by the drag factor $6\pi\mu a$. $\mathbf{E}_z$ is the unit vector. Let us introduce (time-dependent) instantaneous terminal velocity $\mathbf{V}_t(t)$.

$$0 = -\mathbf{R}(\mathbf{x}(t)) \cdot (\mathbf{V}_t(t) - \mathbf{u}^{\infty}) - \mathbf{E}_z \tag{9}$$

Then the equation of motion (8) is

$$\tilde{St}\frac{d}{dt}\mathbf{U}(t) = -\mathbf{U}(t) + \mathbf{V}_t(t). \tag{10}$$

Although $\tilde{St}$ is, in principle, the tensor proportional to the Stokes number $St\mathbf{R}^{-1}$, we approximate it as a scalar constant $\tilde{St}$. This parameter represents the relaxation time of the velocity. We integrate (10) by the 4th order Runge-Kutta method to get the trajectories of particles.

Finally we comment on the calculation of $\mathbf{R}$. It is essential for the hydrodynamic interaction that the fluid is bounded by the vessel (pipe) in the systems considered here. Because the introduction of the boundary as the vessel is hard task to the dynamical simulations, we treat the problems under the periodic boundary condition [11,12].

# 3. SIMULATION RESULTS

## 3.1 Fluidized Beds

In the fluidized beds, the existence of the bottom which support particles are important. In the simulations we introduce fixed particles.

*bubbling flow* [7]

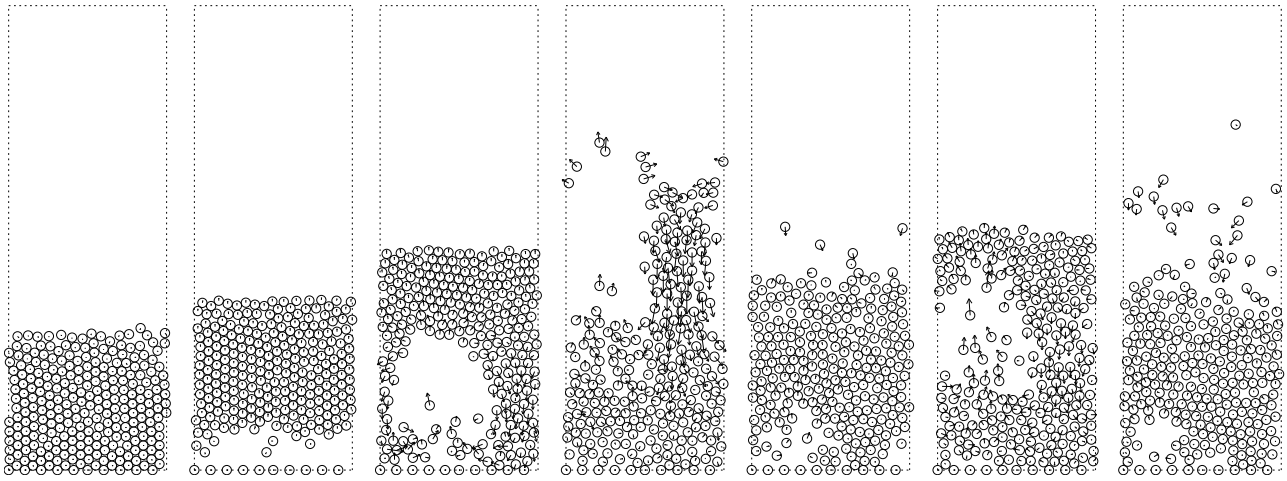

FIG. 2. Sequence of the simulation of a fluidized bed ($N = 256 + 10,\ \tilde{St} = 10,\ u^{\infty} = 0.3$).

The time sequence of the bubbling flow is shown in Fig. 2. The value of $\tilde{St} = 10$ corresponds to the particles with $a = 10^{-3}$[cm], $\rho_p = 2.5$[g cm$^{-3}$] in air.

## *channel flow*

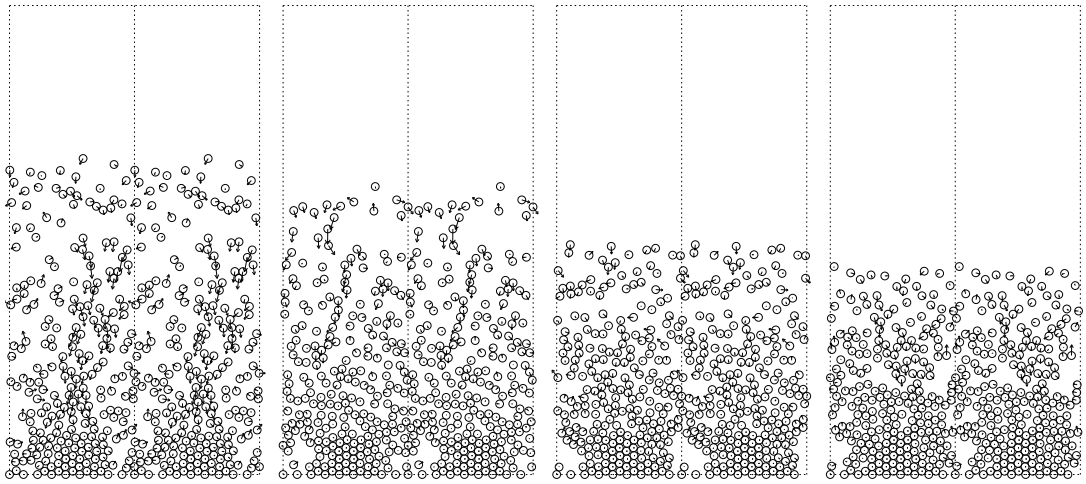

FIG. 3. Sequence of the simulation of a fluidized bed ($N = 231 + 9,\ \tilde{St} = 0.1,\ u^{\infty} = 0.2$).

When $\tilde{St}$ is smaller, the behavior of the system change from "bubbling flow" to "channel flow", where a route of the fluid flow are formed (Fig. 3).

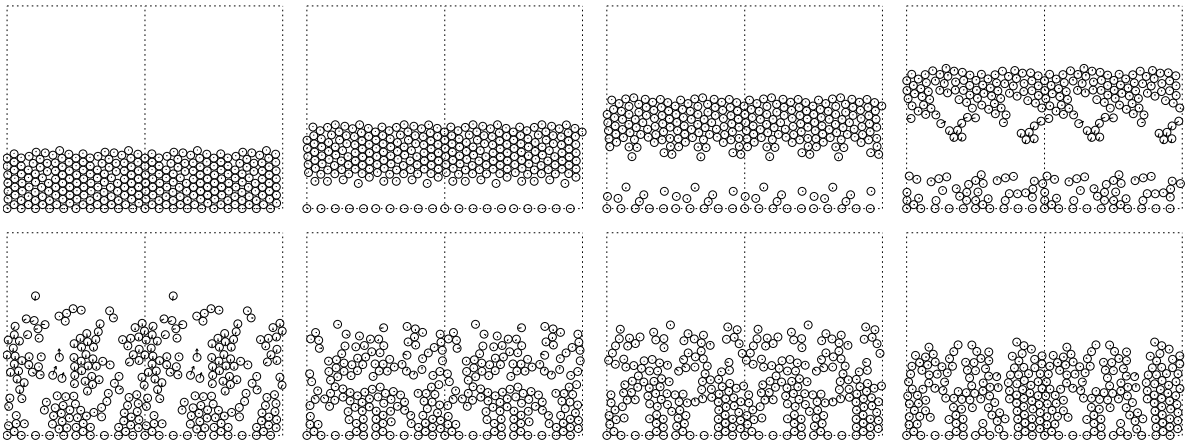

FIG. 4. Sequence of the simulation of a fluidized bed ($N = 128 + 10,\ \tilde{St} = 0,\ u^{\infty} = 0.3$).

The channel flow shows that the systems cannot be fluidized well. This tendency is more obvious in the simulation with $\tilde{St} = 0$ (Fig. 4). In this simulation we can see that particles form a cluster.

## 3.2 Pipe Flow [13]

### *density waves*

To simulate the behavior of pipe flow, we use the narrow periodic cell. We show the time sequence of the simulation in Fig. 5.

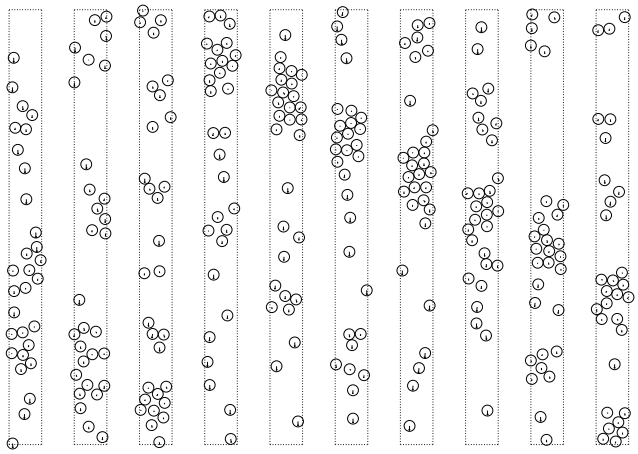

FIG. 5. Sequence of the simulation of pipe flow ($N = 30,\ \tilde{St} = 10$).

TABLE I. The parameters of simulations. $\tilde{St}$ is the effective Stokes number in Eq. (10), $N$ is the number of particles in the unit cell, $L_x$,$L_y$ and $L_z$ are the lengths of the unit cell.

| | $\tilde{St}$ | $N$ | $L_x$ | $L_y$ | $L_z$ |
|---|---|---|---|---|---|
| (a) | 0.0 | 30 | 6 | 2 | 80 |
| (b) | 10.0 | 30 | 6 | 2 | 80 |
| (c) | 100.0 | 30 | 6 | 2 | 80 |
| (d) | 10.0 | 15 | 6 | 2 | 80 |
| (e) | $\infty$ | 30 | 6 | 2 | 80 |

We can see the density waves.

We also simulate with several $\tilde{St}$ as follows.

The spatiotemporal patterns of density are presented in Fig. 6).

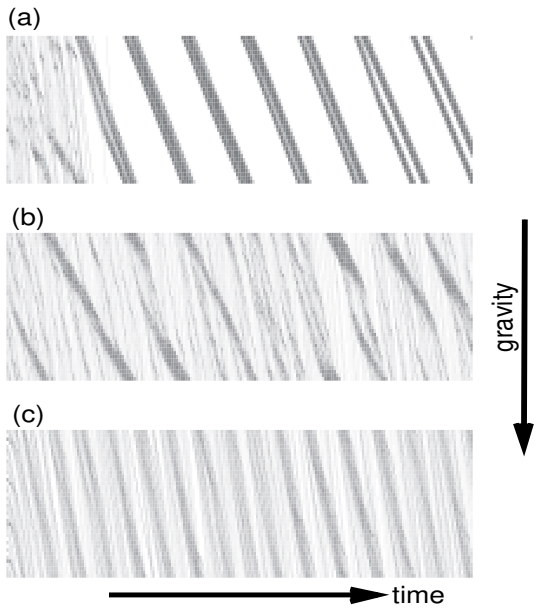


FIG. 6. Spatiotemporal patterns of density with (a) $\tilde{St} = 0$,(b) $\tilde{St} = 10$ and (c) $\tilde{St} = 100$. Dark regions correspond to high densities.

In the case, (a) $\tilde{St} = 0$, particles are fixed as a single cluster, but in other cases, (b) $\tilde{St} = 10$ and (c) $\tilde{St} = 100$, particles are falling through the cluster.

# 4. ANALYSIS

## 4.1 Velocity Distribution Function [7]

In this section we discuss the velocity distribution functions (VDFs). In most of the simulations we can see the non-Gaussian VDFs. It is found that the deviation from Gaussian is closely related to the local density of particles. Let us consider the bubbling flow where particle density largely changes.

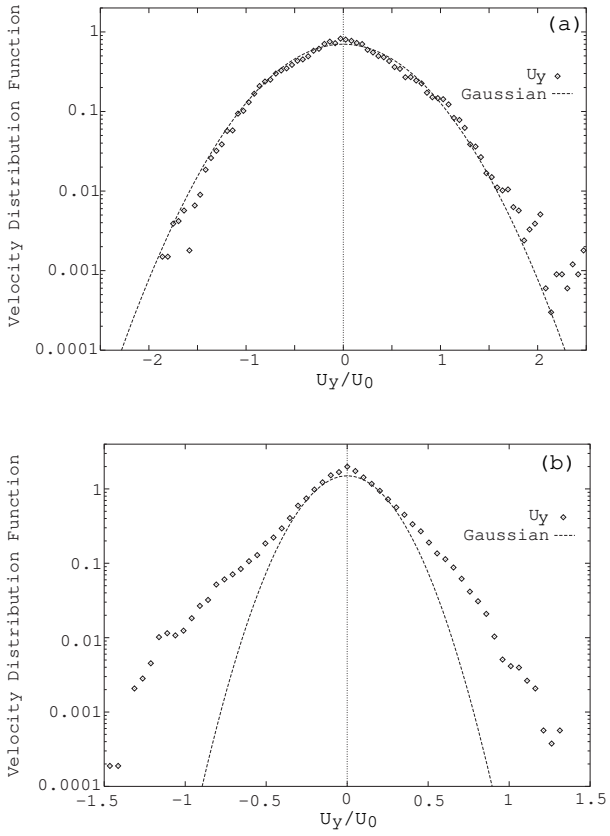


FIG. 7. The velocity distribution functions of bubbling flow in the state (a) with a bubble and (b) without a bubble. These are (a) low and (b) high density state.

Fig. 7 (a) and (b) correspond to the state with and without a bubble respectively. From this results we may indicate that non-Gaussian properties are more obvious in the high density of particles.

## 4.2 Power Spectra of Density Fluctuation [13]

Here we investigate the power spectra of density fluctuations obtained from the simulations of pipe flows.

These spectra are calculated as follows. At first we divide horizontally the unit cell into 20 sub cells and calculate the time series of density in each sub cell. Then we calculate the power spectra of each sub cell by a fast Fourier transform and average them over 20 sub cells.

Frequencies are scaled by $f_0$ which is the lowest frequency.

The simulation (e) is presented as the example with no density waves for comparison, which is performed without the hydrodynamic effects corresponding to the case of $\tilde{St} = \infty$.

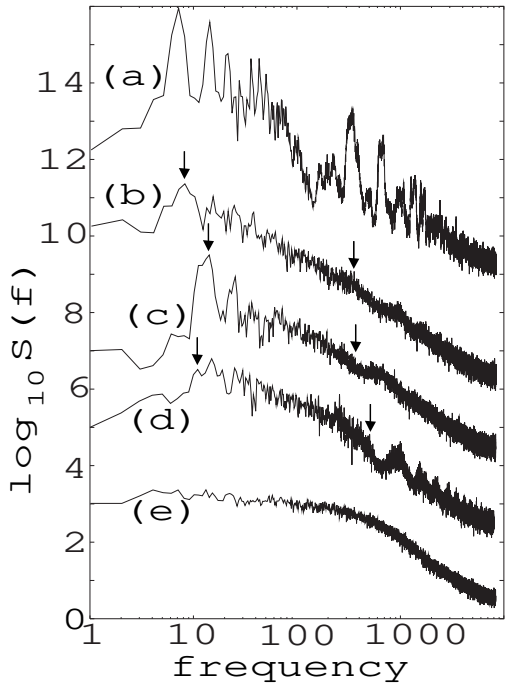


FIG. 8. Power spectra $S(f)$ of density fluctuation of the simulation of pipe flows.

We can see that power laws are observed for the simulations with finite $\tilde{St}$ in the range between $f_c$ and $f_s$, which is defined as

$$f_c = V_c / L_z \tag{11}$$

$$f_s = \bar{V} / 4a \tag{12}$$

where $V_c$ and $\bar{V}$ are the mean velocity of the cluster and the particles respectively, $L_z$ is system size in direction of the gravity and $4a$ is the length of the sub cells used in the calculation of spectra. Therefore $f_c$ and $f_s$ correspond to the return time of cluster and the characteristic time in small scale motion respectively. The exponents in the range are shown in the Table below.

| | $V_c$ | $\bar{V}$ | $f_c$ | $f_s$ | $\alpha$ |
|---|---|---|---|---|---|
| (b) | 0.12 | 0.28 | 8 | 350 | $-1.47 \pm 3 \times 10^{-2}$ |
| (c) | 0.21 | 0.31 | 13 | 380 | $-1.40 \pm 3 \times 10^{-2}$ |
| (d) | 0.18 | 0.43 | 11 | 510 | $-1.32 \pm 3 \times 10^{-2}$ |

This kind of spectra of density fluctuation have been observed in a recent experiment of pipe flow [5]. From the meaning of $f_c$ and $f_s$, it is suggested that the power law reflects the behavior in relatively small scale rather than the cluster itself.

The existence of low-frequency limit may be due to the limit of system size or the periodicity in the simulations.

# 5. DISCUSSION

## 5.1 Simple Model for Power law

From the above analysis of the simulations, it is found that the non-Gaussian VDFs are observed in high density state. From the range of frequency where the power laws in density fluctuations are observed, it is indecated that the dynamics in the cluster is important. To see the dynamics in the cluster occuring in the simulation, we show the velocity of tagged particles in Fig. 9.

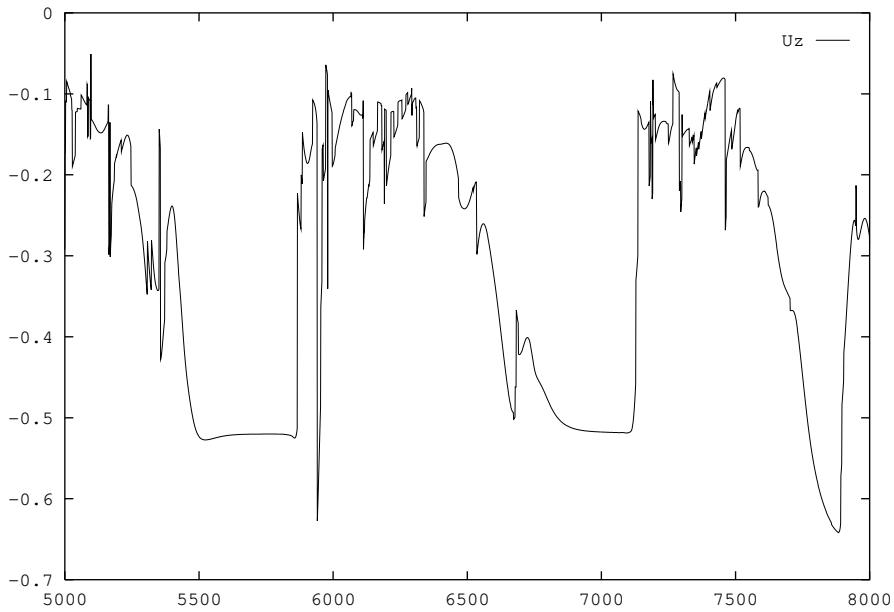


FIG. 9. The time sequence of the velocity of tagged particle.

From this figure the processes in the cluster are collisions and relaxation to the terminal velocity.

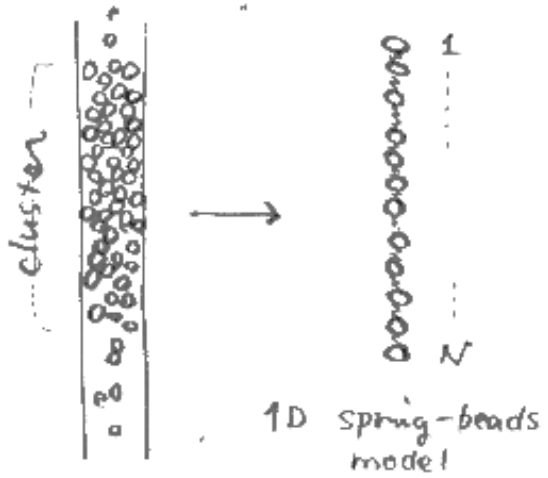


For simplicity we consider 1-dimensional spring-beads model with the friction,

$$m\ddot{r}_n + \zeta\dot{r}_n = k\partial_{nn}r_n \qquad (13)$$

where $n = 1, \cdots, N$ and the resistance coefficient $\zeta$ can be separated into the mean value $\bar{\zeta}$ and fluctuating part $\Delta\zeta$ as follows,

$$\zeta = \bar{\zeta} + \Delta\zeta. \qquad (14)$$

If $\Delta\zeta\ \dot{r}$ could be treated as a noise, this model is reduced to the Rouse model for single polymer [14] and then this predicts that the

dynamic structure factor $g(k,t)$

$$g(k,t) \sim \exp\left[-(t/\tau)^{\beta}\right] \tag{15}$$

with $\beta = 1/2$ for $k > L_c$, where $L_c$ is the cluster size. The exponent $\beta = 1/2$ corresponds to the power spectra of density fluctuation $S(f) \sim f^{-3/2}$ !

# 6. CONCLUSION

In this poster, we construct the simulation method of granular flow with hydrodynamic interaction in the wide range of parameters, that is, the gas-fluidized beds and the liquid-fluidized beds can be simulated in the same scheme. Realistic bubbling flows and channel flows in fluidized beds and the density waves in pipe flows are observed in this method.

From the simulations we find that the non-Gaussian properties are closely related to the density of particles. The power law in the density fluctuations in pipe flow, which observed in experiments [5], are also observed.

From the results of power spectra, the power law is observed in the range between $f_c$ and $f_s$. This means that the power law reflects the dynamics in the cluster.

In the discussion we present a very simple model similar to that in polymer systems. Of course, this picture is insufficient. For example, we assume Gaussian noise *a priori* and the existence of the cluster. These problems are very important to understand the granular flows.

REFERENCES


[1] *Fluidization*, 2nd ed., edited by J. F. Davidson, R. Clift, and D. Harrison (Academic Press, London, 1985).

[2] D. Gidaspow, *Multiphase Flow and Fluidization* (Academic Press, London, 1994).

[3] K. L. Schick and A. A. Verveen, Nature **251**, 599 (1974).

[4] T. Pöschel, J. Phys. I France **4**, 499 (1994).

[5] S. Horikawa, A. Nakahara, T. Nakayama, and M. Matsushita, (1995), submitted to J. Phys. Soc. Jpn.

[6] H. Hayakawa and K. Ichiki, Phys. Rev. E **51**, R3815 (1995).

[7] K. Ichiki and H. Hayakawa, Phys. Rev. E **52**, 658 (1995).

[8] J. Happel and H. Brenner, *Low Reynolds number hydrodynamics* (Martunus Nihhoff, Dordrecht, 1973).

[9] S. Kim and S. J. Karrila, *Microhydrodynamics* (Butterworth-Heinemann, Boston, 1991).

[10] J. F. Brady and G. Bossis, Ann. Rev. Fluid Mech. **20**, 111 (1988).

[11] C. W. J. Beenakker, J. Chem. Phys. **85**, 1581 (1986).

[12] J. F. Brady, R. J. Phillips, J. C. Lester, and G. Bossis, J. Fluid Mech. **195**, 257 (1988).

[13] K. Ichiki, , unpublished (adap-org/9505004).

[14] M. Doi and S. F. Edwards, *The Theory of Polymer Dynamics* (Oxford University Press, Oxford, 1986).